

環状ブラストウェブの流れ構造とそのインパルス性能の数値解析

Numerical Study of Toroidal Blast Wave: Flow Structure and Impulsive Performance on A Spherical Target

○Chongfa Xie, Duc Thuan Tran, 森 浩一 (名大流体研)

○Chongfa Xie, Duc Thuan Tran, Koichi Mori (Nagoya University)

Abstract (概要)

The purpose of this research is to study the impulsive performance of the new system with a numerical method based on Computational Fluid Dynamics (CFD). We focus on the impulsive performance of pulsed-laser induced blast wave on a spherical model under a dense atmosphere, without considering the laser ablation effect. As a result, it is found that toroidal blast wave induced by annular-spot laser pulse has a better impulse capacity than spherical blast wave induced by single-spot laser pulse. Specifically, the effect of shock convergence is also investigated to show the propagation and flow structure of toroidal blast wave. The focusing effect and shock reflection occur when toroidal blast wave converges on the center. These effects guide and accelerate the flow along the central axis, and benefit to total impulse impacted on the target. Other factors that influence total impulse of blast wave are also investigated in this research.

記号の説明

- C_m : momentum coupling coefficient (N/MW)
- $C_{m,bw}$: momentum coupling coefficient when $\eta_{bw}=1$ (N/MW)
- d_L : diameter of single spot laser beam (m)
- $d_{a,i}$: inner radius of annular laser beam (m)
- $d_{a,o}$: outer radius of annular laser beam (m)
- E_{bw} : blast wave energy (J)
- I_m : total impulse impacted on target (N·s)
- p_a : ambient air pressure (Pa)
- R_{bw} : $(E_{bw}/p_a)^{1/3}$ (m)
- R_{sphere} : radius of spherical target (m)
- V_{bw} : blast wave volume (m³)
- η_{bw} : blast wave energy conversion efficiency

1. Introduction

Laser propulsion was proposed in 1970s to realize low-cost space launch¹⁾. An off-board laser energy source was suggested to be used in vehicle propelling. To investigate the feasibility of laser propulsion, Myrabo et al designed an air-breathing pulsed-laser powered vehicle, Lightcraft²⁾ (Fig. 1(a)), and demonstrated several flight tests for laser-powered launching validation, one of which reached a world-record altitude of 71 meters on Oct. 2nd, 2000.³⁾ However, the lightcraft tended to deviate from the laser beam due to laser divergence generated by

attitude angular offset, and was unable to reach a higher altitude.

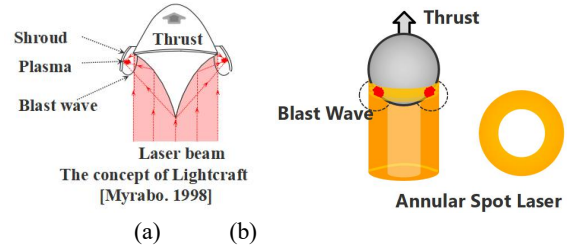


Fig.1 Laser-powered air-breathing blast wave propulsion system

In the previous study, a new laser powered propulsion system, where a spherical capsule is launched by an annular-spot laser beam (see Fig. 1(b)), was proposed to avoid attitude control issues and improve the beam-riding performance⁴⁾. To investigate the feasibility of the new system, the C_m should be formulated specifically as a function for spherical capsule propelled by an annular-spot laser pulse. In dilute atmosphere, impulse mainly originated from laser ablation since there is weak interaction between ablated vapor and ambient gas. In this case, Phipps *et al.*⁵⁾ have established the scaling model of C_m from laser ablation that could be utilized directly. In a dense atmosphere, laser ablation has negligibly small impact on the generated impulse. The impulsive thrust is mainly generated when the laser-induced blast wave expanding outward. Therefore, in our study, we expect to investigate C_m on spherical target as the function of η_{bw} , R_{sphere}/R_L and $(R_{a,i}+R_{a,o})/2R_{sphere}$,

under dense gas, i.e. ambient pressure, $p_a=10\text{kPa}\sim 100\text{kPa}$. Furthermore, the shock focusing happening in the center of toroidal blast wave shows a positive effect in thrust generation. To study the effect of blast wave expansion on total impulse, the flow pattern of toroidal blast wave is also studied on spherical target. In details, Mach reflection and jetting effect occur during the toroidal blast wave convergence.

2. Method

The flow field is investigated through a numerical method for toroidal blast wave induced by annular spot laser. Three-dimensional compressible Euler Equations are used to simulate fluid dynamics of pulsed-laser induced flow. Ambient gas is treated as the ideal gas in the simulation. The Euler equations are discretized spatially by finite volume method and integrated in time with 3-stage Runge-Kutta method. The HLL-family Riemann solvers are used to evaluate the inviscid fluxes with 3rd-order MUSCL high-resolution approach and Von Albada limiter. Outer boundary is set as Riemann Invariant Boundary ⁶⁾ to suppress nonphysical wave reflecting from the boundary. On target surface, the boundary condition is set as slip wall boundary and pressure values were extrapolated from next cells. The computation was performed under CFL=0.5. For computational grid, a spherical mesh using meridians (lines from pole to pole) and parallels (lines parallel to the equator) is adopted on the spherical target. Grid convergence, especially in vertical direction, is checked to make the thrust forcing on the target independent of the grid resolution.

The computational conditions are set according to Table 1. Three cases, single spot laser pulse and two annular spot laser pulses, are simulated. To simplify the laser-ablation processes, explosion source model ⁷⁾ is adopted to simplify the laser-ablation process on the target surface in the simulation. In this method, E_{bw} is assumed in advance; that is, all the blast wave energy E_{bw} is deposited inside a small region V_0 with a high-pressure p_0 in initial conditions when treating the ambient gas as idea gas.

Table 1 Computational parameters of single spot and annular spots

Ambient pressure p_a	10k - 100kPa
Blast wave energy E_{bw}	0.01J - 0.5J
Target radius R_{sphere}	5mm (fixed)
Energy conversion efficiency η_{bw}	1.0
Single spot laser diameter d_L	$1.3 \cdot 10^{-3}$ m
Annular spot laser #1 diameters	$d_{a,i}$ $3.1 \cdot 10^{-3}$ m $d_{a,o}$ $6.5 \cdot 10^{-3}$ m
Annular spot laser #2 diameters	$d_{a,i}$ $7.7 \cdot 10^{-3}$ m $d_{a,o}$ $8.3 \cdot 10^{-3}$ m

Blast wave propagation in a dense atmosphere is dependent on E_{bw} and p_a according to former studies ^{8,9)}. Consequent I_m is first calculated by integrating target surface and time for the

pressure, then C_m is calculated with various E_{bw} under p_a from 10k to 100kPa in each cases of laser pulse. In this research, C_m results are compared among three laser pulse cases with same $\eta_{bw}=1$ to study the relation of C_m and R_{sphere}/R_{bw} . Therefore, we introduced a new parameter, $C_{m,bw}$ defined as

$$C_{m,bw} = \frac{I_m}{E_{bw}} = \frac{C_m}{\eta_{bw}} \quad (1)$$

so that we can omit the influence of energy conversion when evaluating the thrust performance.

3. Results and discussion

Fig. 2 shows the calculation results of $C_{m,bw}$ of various computational conditions, E_{bw} and p_a . In all laser pulse cases, $C_{m,bw}$ is investigated via dimensionless shock wave radius, R_{sphere}/R_{bw} . According to the result, it can be found that the plots of different conditions distribute around the same curve in each case. $C_{m,bw}$ could be determined uniquely by R_{sphere}/R_{bw} for specific laser beam pattern; that is, $C_{m,bw}$ can be formulated as the function of R_{sphere}/R_{bw} , even though it has not been done. Furthermore, $C_{m,bw}$ increases overall as R_{sphere}/R_{bw} increases. Considering the definition of $R_{bw}=(E_{bw}/p_a)^{1/3}$, that is larger $C_{m,bw}$ could be obtained in higher p_a and smaller E_{bw} . It should be noted that there is a peak of $C_{m,bw}$ around $R_{\text{sphere}}/R_{bw}=0.8$ in each of the annular-spot laser pulse. That is because the total impulse impacted on the target is originated from the pressure difference generated by blast wave propagation around the target. As the wave expansion outward, temporal force on the target becomes negative when the blast wave is over-expanded. The negative effect of quasi-vacuum inside the blast wave, respecting to p_a , is larger than the positive effect around the wave front. In high p_a and small E_{bw} , this effect becomes more outstanding and makes I_m smaller. Consequently, $C_{m,bw}$ decrease and a peak appears. In single-spot case, there should also be a peak of $C_{m,bw}$, but it is outside the interval of R_{sphere}/R_{bw} shown in Fig. 2. The peak value could help to find the optimized point of propulsion performance for a specific laser-pulse pattern.

It is obvious that the laser with larger diameter has worse $C_{m,bw}$ than the laser with smaller diameter because of the angular effect from laser position. What interests us is that the $C_{m,bw}$ of both the annular-spot laser pulse are overall larger than that of the single-spot laser pulse in R_{sphere}/R_{bw} interval shown in the result. Also, they increase faster as the R_{sphere}/R_{bw} increasing in the interval of 0.1 to 0.8. One main reason is the shock focusing effect and jetting effect of toroidal blast wave induced by the annular-spot laser pulse.

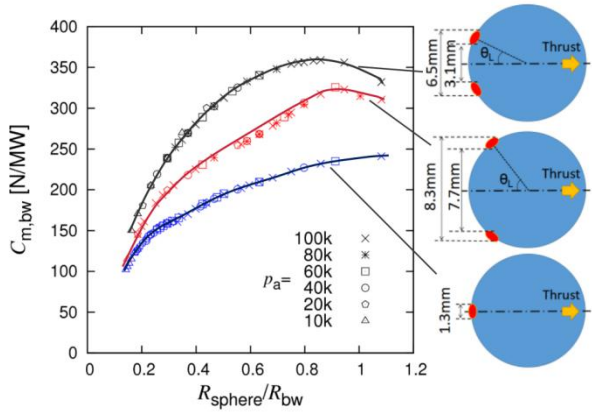
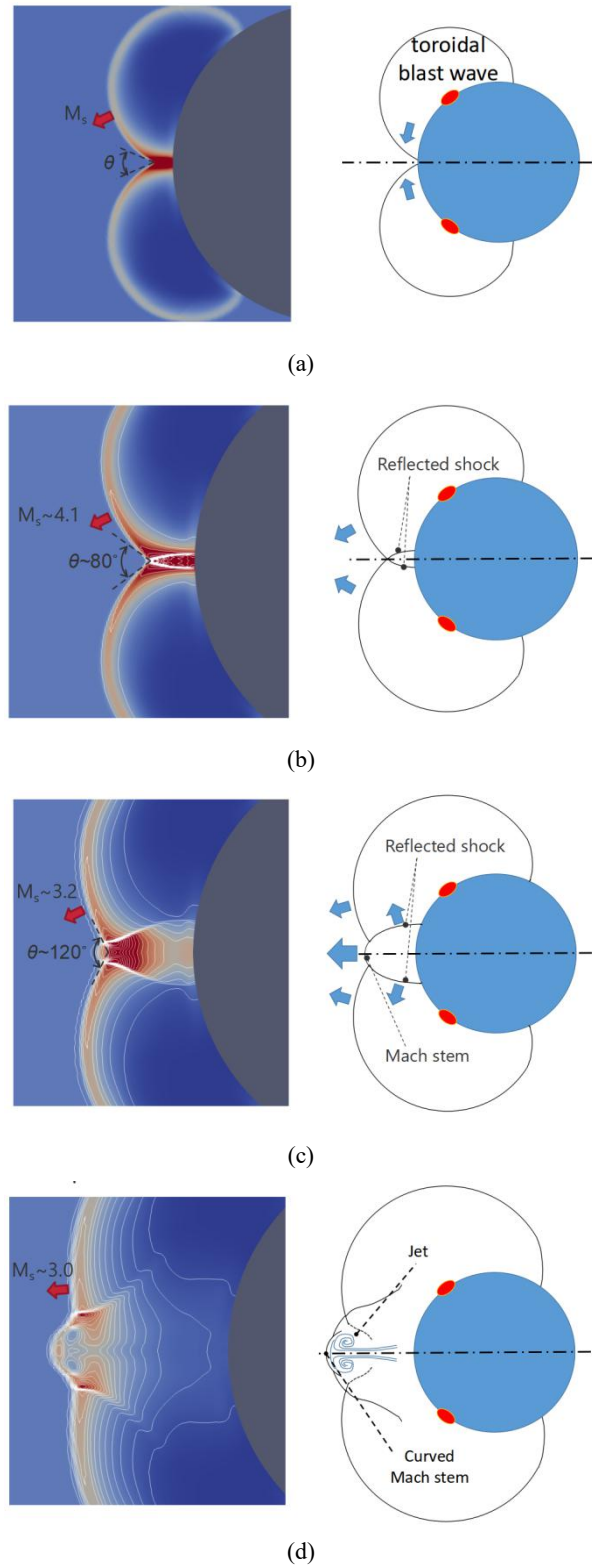


Fig. 2 Simulated C_m vs $R_{\text{sphere}}/R_{\text{bw}}$.

Fig. 3 shows the propagation structure of a toroidal blast wave. When the toroidal blast wave expands outward from laser irradiated spot, its inner part that propagates toward the central axis converges along the axis, see in Fig. 2(b). A locally high-density and pressure region is created since the gas is compressed by the wave convergence. The phenomenon of toroidal shock wave focusing was investigated in former researches experimentally¹⁰⁻¹²⁾ and numerically^{13,14)}. The strong shock wave focuses and results in flow accelerating along the symmetry axis. In early stage of focusing, regular shock reflection happens since the shock-incident angle is small, see Fig. 3(b). As the blast wave expanding outward, a Mach stem occurred in the front of flow and shock reflection pattern transits into Mach reflection, see Fig. 3(c). Based on Mach reflection theory^{15,16)}, Mach stem occurs since the interaction of shock and reflection shock, and the incident angle should be larger than about 80° . Furthermore, it can be found that the Mach stem is curved by a higher speed flow behind it, see Fig. 3(d). To be exact, a jet occurs in the symmetry axis and reforms the Mach stem. The jet appears because of, also, the interaction of shock and reflection shock¹⁷⁾. Similar phenomenon occurring in shock focusing is also found in references^{13,14)}. According to^{16,17)}, flows of post-reflected-shock and the jet have more enthalpy and momentum than the post-flow of Mach stem. The jet draws and guides the higher momentum flow toward the Mach stem. The jet exists in a relative long time according to the simulation result, see Fig. 3(e). In this processes, the guided flow induces a positive impact on the total impulse generated by annular-spot laser pulse. In single-spot case, the energy deposited in the gas generates a blast wave expanding outward uniformly. Respecting to central axis, normal momentum components of the flow have no benefit to the total impulse. Negative effect impacts on total impulse when part of the flow goes along the spherical target surface. As a result, the annular-spot laser pulse shows a better impulse performance than the single-spot laser pulse in the view of $C_{m,bw}$.

In addition, as the blast wave expanding outward, the gas inside the blast wave becomes low density and low pressure.

Because of the pressure vibration behind the blast wave, a secondary shock occurs from the center and induces Richtmyer-Meshkov instability on the high-low density interface, see Fig. 3(e).



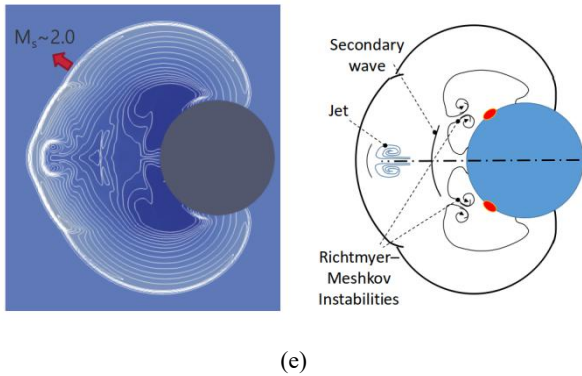


Fig. 3 Density distribution (left: lines show the density contour) and flow structure schematic (right): (a) $t=1.00\mu\text{s}$: strong shock converges in front of the target; locally high density and pressure region resulted from shock focusing; (b) $t=1.13\mu\text{s}$: density contour (line); regular reflection of shock interaction on the center; (c) $t=1.55\mu\text{s}$: Mach reflection of shock interaction on the center; (d) $t=2.54\mu\text{s}$: Jetting effect happens behind the Mach stem; (e) $t=11.6\mu\text{s}$: long existing jet and flow inside the blast wave.

4. Conclusion

A simple numerical method, using explosion source model, was found adaptable to estimate the performance of the annular spot laser powered launch system. $C_{m,bw}$ is able to be formulated as a function of $R_{\text{sphere}}/R_{\text{bw}}$, and to be utilized in impulse estimation in place of C_m . When η_{bw} is the same, C_m by annular footprint are larger than that by single spot under ambient condition $p_a=10\text{kPa}\sim 100\text{kPa}$, due to the toroidal blast wave focusing effect and jetting effect on the central axis. Shock focusing is one of the factors that can improve the impulsive performance of annular spot laser pulse. Furthermore, flow structure of toroidal blast wave convergence was investigated on spherical target. Oblique-shock reflection phenomenon can be used to explain the toroidal blast wave focusing. However, exact conditions have not been clarified for different flow patterns, specifically the occurrence of jet. That will be the future work of our study.

References

- 1) Kantrowitz, A., "Propulsion to Orbit by Ground-Based Lasers," *Astronautics and Aeronautics*, Vol. 10, No. 5, May 1972, pp. 74-76.
- 2) Myrabo, L.N., Messitt, D.G., and Mead, F.B., Jr., "Ground and Flight Tests of a Laser Propelled Vehicle," *AIAA Paper* 98-1001, Jan. 1998
- 3) MYRABO, Leik N. World record flights of beam-riding rocket lightcraft: Demonstration of 'disruptive' propulsion technology. *AIAA paper*, 2001, 3798.2001: A01-34448.
- 4) MORI, K. Laser-Propelled Launch of a Spherical Capsule

Guided by a Donut-Mode Beam. *Journal of Spacecraft and Rockets*, 2017.

- 5) PHIPPS JR, C. R., et al. Impulse coupling to targets in vacuum by KrF, HF, and CO₂ single - pulse lasers. *Journal of Applied Physics*, 1988, 64.3: 1083-1096.
- 6) CARLSON, Jan-Reneé. Inflow/outflow boundary conditions with application to FUN3D. 2011.
- 7) RITZEL, D. V.; MATTHEWS, K. An adjustable explosion-source model for CFD blast calculations. In: *Proc. of 21st International Symposium on Shock Waves*. 1997. p. 97-102.
- 8) MORI, Koichi; MARUYAMA, Ryo; SHIMAMURA, Kohei. Energy conversion and momentum coupling of the sub-kJ laser ablation of aluminum in air atmosphere. *Journal of Applied Physics*, 2015, 118.7: 073304.
- 9) MORI, Koichi; KOMURASAKI, Kimiya; ARAKAWA, Yoshihiro. Energy transfer from a laser pulse to a blast wave in reduced-pressure air atmospheres. *Journal of Applied Physics*, 2004, 95.11: 5979-5983.
- 10) STURTEVANT, B.; KULKARNY, V. A. The focusing of weak shock waves. *Journal of Fluid Mechanics*, 1976, 73.4: 651-671.
- 11) HOSSEINI, S. H. R.; ONODERA, O.; TAKAYAMA, K. Characteristics of an annular vertical diaphragmless shock tube. *Shock Waves*, 2000, 10.3: 151-158
- 12) TENG, H., et al. Numerical investigation of toroidal shock wave focusing in a cylindrical chamber. *Shock Waves*, 2005, 14.4: 299-305.
- 13) BARKHUDAROV, E. M., et al. Reflection of a ring shock wave from a rigid wall. *Shock Waves*, 1994, 3.4: 273-278.
- 14) HONGHUI, Teng; ZONGLIN, Jiang. Gasdynamic characteristics of toroidal shock and detonation wave converging. *Science in China Series G: Physics Mechanics and Astronomy*, 2005, 48.2: 739-749.
- 15) GLASS, Irvine I.; SISLIAN, Jean Pascal. *Nonstationary flows and shock waves* (pp. 180-222). Oxford University Press on Demand, 1994.
- 16) HENDERSON, L. F., et al. The wall-jetting effect in Mach reflection: theoretical consideration and numerical investigation. *Journal of Fluid Mechanics*, 2003, 479: 259-286.